

1 Modeling the ecological status response of rivers to multiple stressors using machine
2 learning: a comparison of environmental DNA metabarcoding and morphological data
3 Juntao Fan ^a, Shuping Wang ^a, Hong Li ^{b,c}, Zhenguang Yan ^{a,*}, Yizhang Zhang ^{a,d}, Xin
4 Zheng ^a, Pengyuan Wang ^a

5 ^a *State Key Laboratory of Environmental Criteria and Risk Assessment, Chinese*
6 *Research Academy of Environmental Sciences, Beijing, 100012, China*

7 ^b *Lancaster Environment Centre, Lancaster University, LA1 4YQ, UK*

8 ^c *UK Centre for Ecology & Hydrology, MacLean Building, Wallingford OX108 BB, UK*

9 ^d *Chinese Research Academy of Environmental Sciences Tianjin Branch, Tianjin,*
10 *300457, China*

11 * Corresponding author.

12 *E-mail address: zgyan@craes.org.cn (Z. Yan).*

13

14 **ABSTRACT**

15 Understanding the ecological status response of rivers to multiple stressors is a
16 precondition for river restoration and management. However, this requires the
17 collection of appropriate data, including environmental variables and the status of
18 aquatic organisms, and analysis via a suitable model that captures the nonlinear
19 relationships between ecological status and various stressors. The morphological
20 approach has been the standard data collection method employed for establishing the
21 status of aquatic organisms. However, this approach is very laborious and restricted to
22 a specific set of organisms. Recently, an environmental DNA (eDNA) metabarcoding
23 data approach has been developed that is far more efficient than the morphological
24 approach and potentially applicable to an unlimited set of organisms. However, it
25 remains unclear how well eDNA metabarcoding data reflects the impacts of
26 environmental stressors on aquatic ecosystems compared with morphological data,
27 which is essential for clarifying the potential applications of eDNA metabarcoding data
28 in the ecological monitoring and management of rivers. The present work addresses this
29 issue by modeling organism diversity based on three indices with respect to multiple
30 environmental variables in both the catchment and reach scales. This is done by
31 corresponding support vector machine (SVM) models constructed from eDNA
32 metabarcoding and morphological data on 24 sampling locations in the Taizi River
33 basin, China. According to the mean absolute percent error (MAPE) between the
34 measured diversity index values and the index values predicted by the SVM models,
35 the SVM models constructed from eDNA metabarcoding data (MAPE = 3.87) provide
36 more accurate predictions than the SVM models constructed from morphological data
37 (MAPE = 28.36), revealing that the eDNA metabarcoding data better reflects
38 environmental conditions. In addition, the sensitivity of SVM model predictions of the

39 ecological indices for both catchment-scale and reach-scale stressors is evaluated, and
40 the stressors having the greatest impact on the ecological status of rivers are identified.
41 The results demonstrate that the ecological status of rivers is more sensitive to
42 environmental stressors at the reach scale than to stressors at the catchment scale.
43 Therefore, our study is helpful in exploring the potential applications of eDNA
44 metabarcoding data and SVM modeling in the ecological monitoring and management
45 of rivers.

46 *Keywords*

47 Machine learning; Modeling; Environmental DNA; Biomonitoring; Freshwater
48 ecosystem

49

50 **1. Introduction**

51 River ecosystems are impacted by multiple environmental variables at both the
52 catchment scale and reach scale simultaneously, and any of these variables lying outside
53 of their normal range can become a stressor. These natural and anthropogenic stressors
54 always interact and are directly or indirectly impacting ecological status (Mori et al.,
55 2019; Romero et al., 2018). For example, catchment scale stressors, such as increased
56 impervious land use by humans, alter physical and chemical conditions of rivers such
57 as increased nutrition through hydrological processes, affecting the structure and
58 function of aquatic ecosystems (Bernhardt et al., 2012; Von Schiller et al., 2017). Here,
59 aquatic communities play an important role in supporting ecosystem services, stability,
60 and biodiversity, and their status can reflect the long-term cumulative effects of
61 environmental stressors on aquatic ecosystems (Franzo and Del Negro, 2019).
62 Therefore, biomonitoring is essential for assessing the impacts of human disturbance at
63 the multiple scales of river basins. The standard approach that has been applied to river
64 biomonitoring involves the sorting and morphological identification of aquatic
65 communities, which is time-consuming and demands a high degree of taxonomic
66 expertise (Pawlowski et al., 2018). However, the high-throughput amplicon sequencing
67 of environmental DNA (eDNA) has recently provided a viable option for biomonitoring,
68 which purified from substrates such as soil or water contains DNA fragments
69 originating from organisms present in that environment (Cordier et al., 2017; Jarman et
70 al., 2018; Mize et al., 2019; Visco et al., 2015). Moreover, a number of previous studies
71 have shown that eDNA metabarcoding data can provide an accurate indication of
72 environmental changes. For example, the relative abundance of operational taxonomic
73 units (OTUs) indicative of plankton was demonstrated to have a significant negative
74 correlation with river nutrient levels (Li et al., 2018a). The foraminifera diversity

75 inferred from eDNA metabarcoding data was found to have a significant positive
76 correlation with the biodiversity in the benthic zone impacted by fish farming activities
77 (He et al., 2019), and the distance from a wellhead in the ocean (Laroche et al., 2016).
78 Benthic macroinvertebrates diversity inferred from eDNA metabarcoding data were
79 also used to assess the freshwater quality (Fernandez et al., 2018; Hering et al., 2018).
80 In addition, previous studies have shown that, compared with morphological
81 classification, eDNA metabarcoding is a relatively simple and affordable method for
82 assessing biodiversity on a large temporal and spatial scale without the need for time-
83 consuming microscopy analysis by experts (He et al., 2019; Ji et al., 2013). Taxonomic
84 classification based on eDNA metabarcoding is usually more accurate than
85 morphological identification, particularly for species with similar morphology and
86 species with poor life cycle characteristics (He et al., 2019; Humbert et al., 2010).
87 Furthermore, eDNA metabarcoding data can be easily reanalyzed to make it suitable
88 for review by third parties (Ji et al., 2013). However, it remains unclear how well eDNA
89 metabarcoding data reflects the impacts of environmental stressors on aquatic
90 ecosystems in comparison with morphological identification data. Clarifying this issue
91 will illuminate potential applications of eDNA technology in the monitoring and
92 management of aquatic ecosystems.

93 Understanding the response of river ecosystems to multiple stressors and identifying
94 important stressors are prerequisites for conducting effective river restoration and
95 management (Meissner et al., 2019; Zhang, 2019). Developing this understanding
96 requires the analysis of biomonitoring data via a suitable model that captures the
97 relationships between the status of ecosystems and various stressors. However, the
98 interactions of multiple stressors produce a combined effect that can be equal to
99 (additive), greater than (synergistic), or less than (antagonistic) the sum of each single

100 effect (Piggott et al., 2015). Indeed, the response of aquatic ecosystems to multiple
101 stressors is typically nonlinear, which greatly complicates the development of accurate
102 models (Jones et al., 2017). The modeling of nonlinear responses can be conducted
103 using various methods, including mathematical/physical models, statistical models, and
104 data-driven models (Al-Mukhtar, 2019; Choubin et al., 2018; Park et al., 2015).
105 However, the complexity of relationships between ecological status and multiple
106 stressors limits the application of mathematical/physical models, and statistical models
107 also suffer from disadvantages, such as poor generalizability due to relatively small
108 sample sizes (Cui and Gong, 2018; Varoquaux, 2018). The development of machine
109 learning (ML) over the past few years has provided a new approach for quantifying
110 these nonlinear relationships (Torija and Ruiz, 2015). At present, ML models have been
111 widely used in the prediction of environmental or ecological indicators. For example, a
112 Bayesian belief network (BBN) was applied to model the combined effects of land use
113 change and climate change on the status of macroinvertebrates and fish in freshwater
114 bodies (Olson, 2018). In addition, artificial neural networks (ANNs), the support vector
115 machine (SVM) and generalized regression neural network, were used for predicting
116 chlorophyll-a concentrations in freshwater, and the results demonstrated that these data-
117 driven ML methods achieved better prediction performance than conventional
118 statistical methods (Marvuglia et al., 2015; Park et al., 2015). The SVM method is
119 particularly advantageous for modeling nonlinear response relationships because the
120 SVM is good for solving high-dimensional and nonlinear problems, while avoiding the
121 difficulties associated with determining the network structure and local minima of the
122 solutions, and provides good generalizability and relatively good prediction
123 performance under small sample size conditions (Vapnik, 1999). These advantages have
124 made SVM outperform other ML methods, e.g., standard ANNs, random forest (RF)

125 classifiers, and boosted trees (BT) classification, in the prediction of soil organic carbon,
126 clay content, and pH (Rossel and Behrens, 2010; Were et al., 2015) and chlorophyll-a
127 (Park et al., 2015) in some regions. Therefore, the SVM is well suited for modeling the
128 relationships between the ecological status of rivers and multiple stressors.

129 The present study compares the ability of eDNA metabarcoding data and
130 morphological identification data to reflect the nonlinear impact of multiple
131 environmental stressors on aquatic ecosystems by employing both sets of data in SVM
132 models corresponding to three ecological indices (i.e. observed species, Shannon
133 Wiener index, and Simpson index), which were commonly used in biodiversity
134 assessment inferred from eDNA metabarcoding or morphological data. As such, the
135 present work helps to explore the potential applications of eDNA technology in the
136 monitoring and management of aquatic ecosystems. In addition, the sensitivity of SVM
137 model predictions of the ecological indices to individual catchment-scale and reach-
138 scale stressors is evaluated, and the stressors having the greatest impact on the
139 ecological status of rivers are identified.

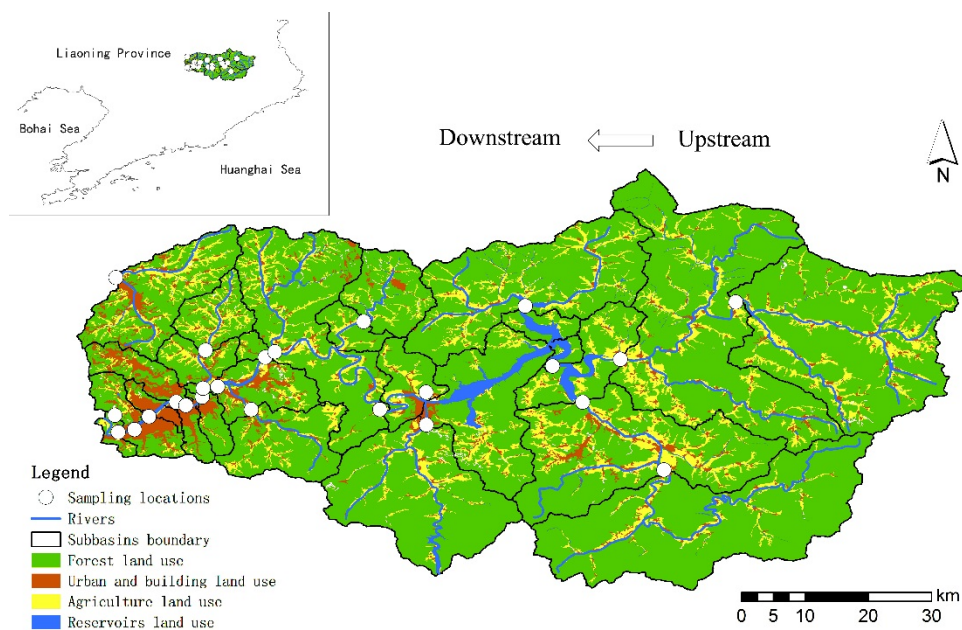
140

141 **2. Materials and methods**

142 *2.1. Study area*

143 The study area was the upstream area of the Taizi River basin (122°23'E–122°53'E,
144 40°28'N–41°39'N) in northeastern China. The location and characteristics of the study
145 area are illustrated in Fig. 1. A previous study demonstrated that the ecological status
146 of the Taizi River in this area was relatively good because the majority of the land in
147 the upstream area was covered by forests, and the intensity of human activities was
148 relatively low (Fan et al., 2015). The primary aquatic organisms of the Taizi River,
149 particularly those species most sensitive to environmental stressors, such as clean-type

150 fishes (*Lampetra morii* and *Odontobutis Obscurus*) and macrobenthos (*Epeorus melli*
151 and *Cambaroides dauricus*), are mainly distributed in the upper reaches of the river. All
152 of these organisms play an important role in maintaining the health of the aquatic
153 ecosystem. However, the urbanization process in the region and the acceleration of
154 human activities in recent years, such as agriculture and mining, have resulted in water
155 shortages, the deterioration of water quality, habitat damage, loss of biodiversity, and
156 the reduction of ecological functions.



157
158 **Fig. 1.** Map of the study area incorporating the upper area of the Taizi River basin at
159 the time of sample collection in October, 2018. The 24 sampling sites and different
160 types of land use in the sub-basins are indicated, and the location of the study area
161 relative to the national boundary of China is shown in the inset.

162
163 *2.2. Ecological and environmental data collection*

164 The 24 sites sampled during October 2018 (Fig. 1) were located in the mainstem and
165 tributaries of the upstream area of the Taizi River basin. Surface water was sampled
166 using sterile bottles. One liter per site was used for eDNA metabarcoding analysis.

167 Three independent extractions of 300 mL were obtained from each one-liter water
168 sample within 6 h after sampling by filtering across a Millipore 0.22 μm hydrophilic
169 nylon membrane. The membrane discs containing captured eDNA were placed in 5.0
170 mL centrifugal tubes, and were instantly frozen and stored at -20°C until DNA
171 extraction. For morphological identification, phytoplankton samples were collected at
172 each sampling site by dragging a nylon mesh with a pore size of 64 μm under the water
173 surface for about 2 min. The water sample concentrated in the drip tube of the net was
174 collected in a 50 mL sample bottle and fixed using Lugol's solution.

175 Environmental variables considered include catchment-scale variables (i.e., land use
176 data) and reach-scale variables (i.e., physicochemical parameters). Land use data were
177 extracted from an analysis of Spot Image data obtained with a 2.5 m resolution. The
178 proportion of land use types (i.e., forest, agriculture, urban, and industrial) was
179 determined for the region of the catchment upstream of each sampling site contributing
180 to the sample characteristics and for a 250 m impact zone adjacent to the studied river
181 segment. Ten physicochemical indicators were selected, including electrical
182 conductivity (EC), dissolved oxygen (DO), pH, biological oxygen demand over 5 days
183 (BOD_5), permanganate index (COD_{Mn}), total phosphorus (TP), ammonia nitrogen
184 concentration ($\text{NH}_3\text{-N}$), total nitrogen (TN), suspended sediment (SS), and volatile
185 phenol (VP). The work of (Fan et al., 2015) and Chinese Quality Standards for Surface
186 Water Resources (Ministry of Water Resources, 1994) established thresholds not to be
187 exceed to assure high ecological status for these physicochemical parameters. These are
188 given as follows: $\text{EC} = 400 \mu\text{s}/\text{cm}$, $\text{DO} = 7.5 \text{ mg}/\text{L}$, $\text{BOD}_5 = 3 \text{ mg}/\text{L}$, $\text{COD}_{\text{Mn}} = 2 \text{ mg}/\text{L}$,
189 $\text{NH}_3\text{-N} = 0.15 \text{ mg}/\text{L}$, $\text{TN} = 0.2 \text{ mg}/\text{L}$ (which was only considered in lake or reservoir
190 samples), $\text{TP} = 0.02 \text{ mg}/\text{L}$, $\text{VP} = 0.002 \text{ mg}/\text{L}$, $\text{SS} = 20 \text{ mg}/\text{L}$, $\text{pH} = 6.5\sim 8.5$.

191

192 *2.3. eDNA metabarcoding and morphological identification*

193 Phytoplankton is the target taxonomic group of eDNA metabarcoding and
194 morphological identification. Total eDNA was extracted using the cetyl
195 trimethylammonium bromide (CTAB) method combined with the Zymo DNA Clean &
196 Concentrator kit (Zymo Research Corp, Irvine, USA) (Yuan et al., 2015). The
197 concentration of eDNA was determined using a NanoDrop One microvolume
198 ultraviolet-visible (UV-vis) spectrophotometer (Thermo Fisher Scientific, Carlsbad,
199 USA). The eDNA was used as templates for the polymerase chain reaction (PCR)
200 method with 18S rRNA gene primers 18SV9F (5'-CCCTGCCNTTTGTACACAC-3')
201 and 18SV9FR (5'-CCTTCNGCAGGTTCACCTAC-3') (Amaral-Zettler et al., 2009; De
202 Vargas et al., 2015). The 18S rRNA gene primers were used because phytoplankton
203 diversity including the cryptic diversity in environmental samples can be indicated by
204 sequencing of 18S rRNA gene, and the SILVA datasets offered the 18S primer
205 opportunity to assess distribution patterns of phytoplankton species (Treusch et al.,
206 2012). The purified PCR products were added with 8-base sequence tags corresponding
207 to each sample. High throughput sequencing was conducted using a MiSeq sequencing
208 platform (Illumina, San Diego, USA). All low-quality sequencing data points with
209 adaptors, ambiguous bases, low complexity, and those having average quality scores
210 less than 20 were discarded using the UPARSE pipeline (Edgar, 2013). The OTUs were
211 determined at the $\geq 97\%$ identity level (Edgar, 2013). Taxonomic annotation analysis
212 was performed using the Qiime2 pipeline (Caporaso et al., 2010) with respect to the
213 SILVA-119 reference database. The remaining high-quality data were transformed to
214 relative proportions before conducting subsequent statistical analysis.

215 For morphological identification, samples were concentrated and precipitated, and
216 the sample volume was adjusted to 20–50 mL. The concentrated sample was then

217 shaken uniformly, and 0.1 mL of the sample was immediately placed in a counting box
 218 for morphological identification. The phytoplankton taxa in each sample were
 219 identified under a 10 × 40 microscope. However, if a high concentration of diatoms
 220 were observed, the sample was sealed and identified under a 10 × 100 microscope. The
 221 specimens were identified to species level through microscopy and taxonomic experts
 222 consultation. The reference used to identify phytoplankton is the Freshwater Algae of
 223 China – Systematics, Taxonomy and Ecology (Hu and Wei, 2006).

224

225 *2.4. SVM model development*

226 The ecological status of the samples was evaluated according to the obtained eDNA
 227 metabarcoding and morphology identification data based on three widely used
 228 ecological indices, i.e., observed species (Kefford et al., 2011), Shannon Wiener index
 229 (Strong, 2016), and Simpson index (Keylock, 2005). The abbreviations and ecological
 230 significance of each of these indices are listed in Table 1. The values for these ecological
 231 indices obtained from the eDNA metabarcoding and morphology identification data
 232 were employed as the response/dependent variables in their respective SVM models.
 233 The catchment-scale variables and reach-scale variables were input to the respective
 234 SVM models as the independent variables.

235

236 **Table 1**

237 List of ecological indices with abbreviations and ecological significance.

Ecological index/Response variables	Abbreviations in eDNA metabarcoding	Abbreviations in morphological identification	Ecological significance
Observed species	Species_E	Species_M	Number of species or OTU observed.
Shannon Wiener index	Shannon_E	Shannon_M	The species/OTUs richness and evenness of the community, but predominantly sensitive to richness.

Richness increases with increasing index value.

Simpson index	Simpson_E	Simpson_M	
			The species/OTUs richness and evenness of the community, but predominantly sensitive to evenness. Evenness increases with increasing index value.

238

239 The SVM was applied for nonlinear regression analysis to establish the response of
240 the ecological indices to the multiple environmental variables. Here, the input data were
241 mapped initially into a higher-dimensional feature space via a kernel function (i.e., a
242 linear kernel, polynomial kernel, radial basis kernel, and Gaussian kernel), and then
243 linear regression was performed in the high-dimensional feature space to obtain the
244 nonlinear regression effect in the original space (Balfer and Bajorath, 2015; Bouboulis
245 et al., 2015). The specific kernel function applied was selected by cross-validation
246 (Piette and Moore, 2018).

247 The regression performance of the SVM depends on the appropriate selection of
248 parameter values, including cost (c), epsilon (ϵ), and gamma (γ), where both c and ϵ are
249 employed to establish the penalty coefficient, which represents the error tolerance of
250 the regression analysis, and γ determines the distribution of the data after it is mapped
251 to the new feature space. Here, the number of support vectors decreases with increasing
252 γ , which affects the speed of training and prediction. The values of these parameters are
253 optimized using a loop traversal algorithm (Cherkassky and Ma, 2004). Normalization
254 was applied to all independent variables to ensure that the indicator values were
255 comparable.

256 The generalization ability of the model was verified by 8-fold cross validation, where
257 the dataset was divided into 8 subsets, and each subset was employed as the testing set
258 once, while the remaining 7 subsets were used as the training set. Accordingly, this

259 process was repeated 8 times. The prediction error of each model was evaluated based
260 on the mean absolute percent error (MAPE), which is calculated for n samples as
261 follows:

$$262 \quad \text{MAPE} = \sum_{t=1}^n \left| \frac{\text{Observed}_t - \text{Predicted}_t}{\text{Observed}_t} \right| \times \frac{100}{n} \quad (1)$$

263 where Observed_t is the observed value and Predicted_t is the predicted value. Then, the
264 model with the smallest MAPE value was selected as the optimal model.

265 Sensitivity analysis was applied to determine the environmental variables that most
266 greatly influenced the model predictions of the ecological indices. This was conducted
267 using the one-factor-at-a-time (OAT) approach. Here, the MAPE values of the model
268 predictions were obtained with one environmental variable omitted at a time, while the
269 other environmental variables were held constant. Then, the impact of each
270 environmental variable on the model prediction was evaluated according to the absolute
271 value of the difference between the MAPE obtained with and without that variable,
272 which is denoted herein as ΔMAPE . Accordingly, the sensitivity of the ecological index
273 predictions to an environmental variable increases with increasing ΔMAPE .

274

275 **3. Results**

276 *3.1. Environmental conditions in catchment and reach scales*

277 All the environmental variables have become stressors, which are marked with “+”
278 in Table 2. Spatial analysis showed that almost all sites were under the selected
279 catchment-scale stressors, and the downstream sites (e.g., s19, s15 and s22) were under
280 more reach-scale stressors than the upstream sites (Table 2). We note that the proportion
281 of forest land use in the catchment scale (0.268–0.910) is greater than that in the 250 m
282 buffer zone (0.092–0.566). However, the proportion of agriculture land use in the 250
283 m buffer zone (maximum value of 0.596) is greater than that in the catchment scale

284 (maximum value of 0.265), which indicates that agricultural disturbance is greater in
 285 the riparian zone than at the catchment scale, while urban and industrial disturbances
 286 have opposite behaviors. Table 2 also indicates that, TN and VP were the reach-scale
 287 variables with the highest number of sites exceeding the thresholds.

288

289 **Table 2**

290 List of environmental variables included in the modeling and spatial distribution of sites
 291 with corresponding stressors. Stressors, i.e., catchment-scale variables impacted by any
 292 artificial land use types (i.e., agriculture, urban and industrial land use), and reach-scale
 293 variables with values less than or greater than the threshold values representing high
 294 environmental status established by the work of (Fan et al., 2015) and Chinese quality
 295 standards for surface water resources (Ministry of Water Resources, 1994), are marked
 296 with “+”.

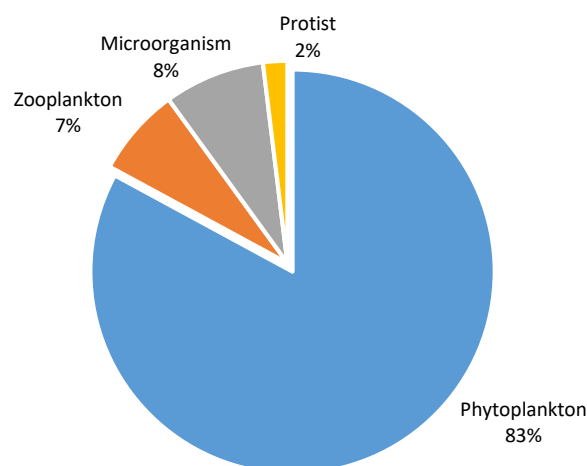
Environmental variables		Abbreviations (Units)	Ranges	Sites with corresponding stressors
Catchment-scale variables				
Forest land use (catchment scale)	+	F_cat (proportion)	0.268–0.910	All sites
Forest land use (250 m buffer zone)	+	F_buf (proportion)	0.092–0.566	All sites
Agriculture land use (catchment scale)	+	A_cat (proportion)	0.018–0.265	All sites
Agriculture land use (250 m buffer zone)	+	A_buf (proportion)	0.000–0.596	All sites except s19, s21, s16, s20
Urban and industrial land use (catchment scale)	+	U_cat (proportion)	0.016–0.646	All sites
Urban and industrial land use (250 m buffer zone)	+	U_buf (proportion)	0.011–0.520	All sites
Reach-scale variables				
Electrical conductivity	+	EC ($\mu\text{s}/\text{cm}$)	142.47–655.33	s19, s13, s14, s21, s15, s17,

				s20, s22
Dissolved oxygen	+	DO (mg/L)	7.02–14.26	s22
pH	+	pH	7.84–8.98	s19, s12, s10, s02, s20
Permanganate index	+	COD _{Mn} (mg/L)	0.48–5.72	All sites except s10, s03, s11
Five-day biochemical oxygen demand	+	BOD ₅ (mg/L)	0.75–8.41	s04, s14, s15, s16, s18, s24
Ammonia nitrogen	+	NH ₃ -N (mg/L)	0.12–3.87	All sites except s05, s03, s07, s06, s01, s02
Total nitrogen	+	TN (mg/L)	1.55–6.75	All sites
Total phosphorus	+	TP (mg/L)	0.004–0.223	s19, s04, s14, s06, s21, s23, s15, s09, s16, s24, s20, s22
Suspended sediment	+	SS (mg/L)	1.56–35.33	s15, s01, s08
Volatile phenol	+	VP (mg/L)	0.004–0.112	All sites

297

298 *3.2. Ecological status derived from eDNA metabarcoding and morphological data*

299 A total of 67 18S rRNA gene libraries were analyzed according to the methodology
300 presented in Subsection 2.3, which resulted in a total of 2,305,498 high-quality
301 sequences, and a total of 6,635 OTUs. The number of OTUs in each sample was
302 distributed between 477–2,661 (Table S1). The result of taxonomic group distribution
303 of OTUs showed that approximately 83% eukaryotic sequences were annotated as
304 phytoplankton (Fig. 2), which confirmed that the phytoplankton can be indicated by
305 sequencing of 18S rRNA gene. Therefore, the eDNA metabarcoding data and
306 morphological data are comparable in this study.



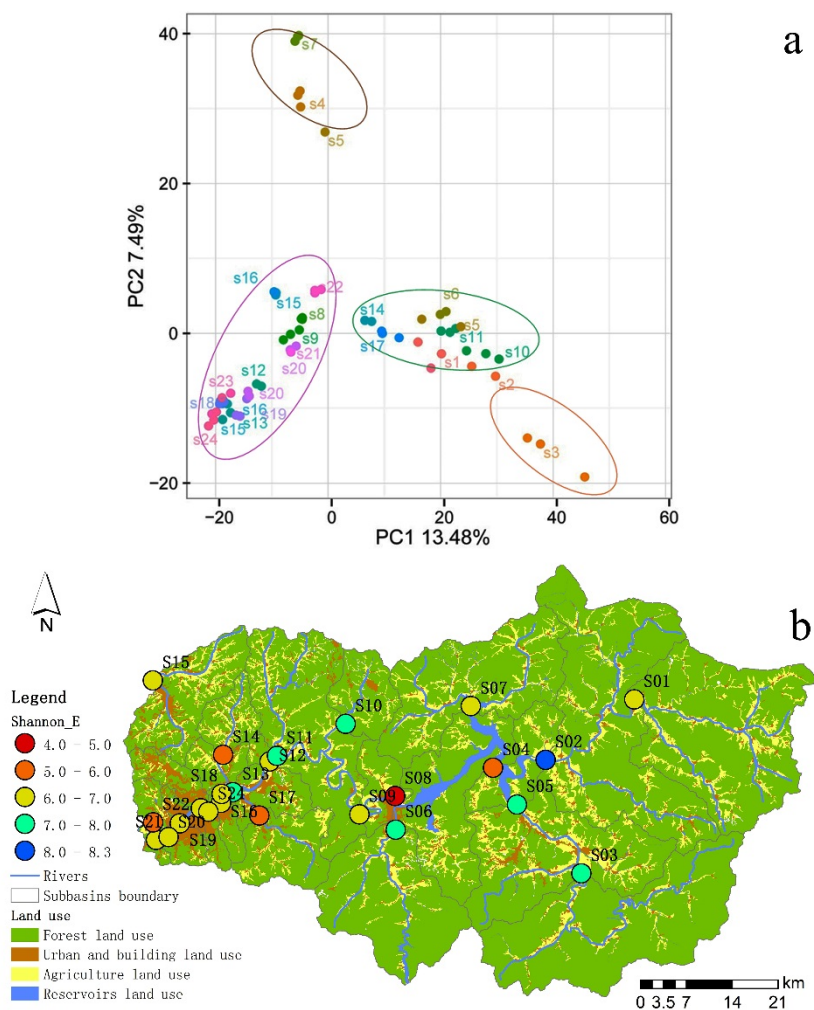
307

308 **Fig. 2.** Percentage of the sequences assigned to each of taxonomic groups.

309 An analysis of the relative abundances of the top 15 orders and families of organisms
 310 for the three replications of the 67 samples were shown in Fig. S1 and S2, respectively.
 311 However, approximately 70% of sequences cannot be assigned to genus level because
 312 the limitation of reference information in the SILVA database. Analysis of top 15
 313 families of organisms indicated that the Mediophyceae, Ochromonadales and
 314 Chlorodendrales accounted for approximately 17.5%, 9.9% and 5.4% of all taxa,
 315 respectively. Analysis of variance (ANOVA) results indicated that no significant
 316 differences were observed for the relative family abundances among the sample
 317 replications ($p > 0.05$).

318 The OTU compositions of the different samples were analyzed according to beta
 319 diversity to reflect differences between samples using principal component analysis
 320 (PCA). Here, PCA uses variance decomposition to reflect the differences between
 321 multiple sets of data on a two-dimensional coordinate graph, where the coordinate axes
 322 are two eigenvalues that reflect the variance to the greatest extent. As such, samples
 323 with similar compositions were clustered in the PCA graph, as shown in Fig. 3A based
 324 on the sampling locations illustrated in Fig. 3B, which also showed the Shannon_E
 325 values for the individual sampling locations and the land use types of the study area.

326 The results indicated that significant differences exist between the sampling sites of
 327 upstream tributaries (e.g., s3, s2 and s1) and the sampling sites of the middle and lower
 328 mainstem, while differences were also observed between the urban (e.g., s22, s21, and
 329 s19) and mountainous sections (e.g., s6, s2, and s5) of the mainstem. However, the some
 330 sites were impacted by the reservoir located in the mainstem of upstream (e.g. s04 and
 331 s08). The spatial distribution of Shannon_E values presented the same pattern, where
 332 the Shannon_E value tended to gradually decrease with increasing disturbance from
 333 human activity from the upstream to the downstream regions, as reflected by increasing
 334 urban and industrial land use.
 335



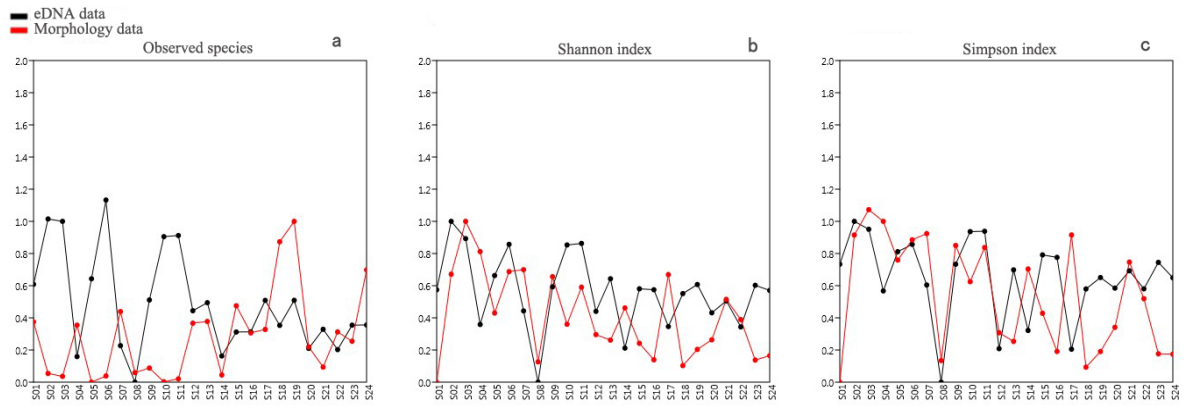
336
 337 **Fig. 3.** (a) Principal component analysis graph for all samples based on the beta

338 diversity derived from eDNA metabarcoding data and (b) the spatial distribution of
339 ecological status based on the Shannon Wiener index.

340

341 The diversity values measured according to the observed species, Shannon Wiener
342 index, and Simpson index derived from eDNA metabarcoding and morphological
343 identification data were normalized and compared, and the results were given in Fig.
344 4A, B, and C, respectively, for sample locations s01–s24. The results in Fig. 4A
345 indicated that in most sites, the observed species values obtained based on eDNA
346 metabarcoding were higher than the values based on morphological data, because OTUs
347 contained a greater number of taxa information. This difference decreased in the
348 Shannon Wiener and Simpson index values, which demonstrated that the data obtained
349 by the two methods reflect similar richness and evenness characteristics of community
350 composition in most sampling sites (Fig. 4B and C). Fig. 4A also showed that 8 sites
351 out of 24 were higher for morphological data than eDNA metabarcoding data, and most
352 of these sites are located in the downstream of study area (e.g. s15, s18, s19 and s24),
353 where a large number of *Cyclotella meneghiniana* were detected in morphological data.
354 *Cyclotella meneghiniana* is a typical indicator of water pollution (Duong et al., 2008).
355 This was proved by Fig. 4B and C, which showed that the Shannon and Simpson indices
356 derived from morphological data were relatively low at these downstream sites.
357 However, the ecological indices derived from eDNA data showed better consistency at
358 these sites, which indicated that the difference between eDNA metabarcoding and
359 morphological data may become larger in polluted river sections.

360



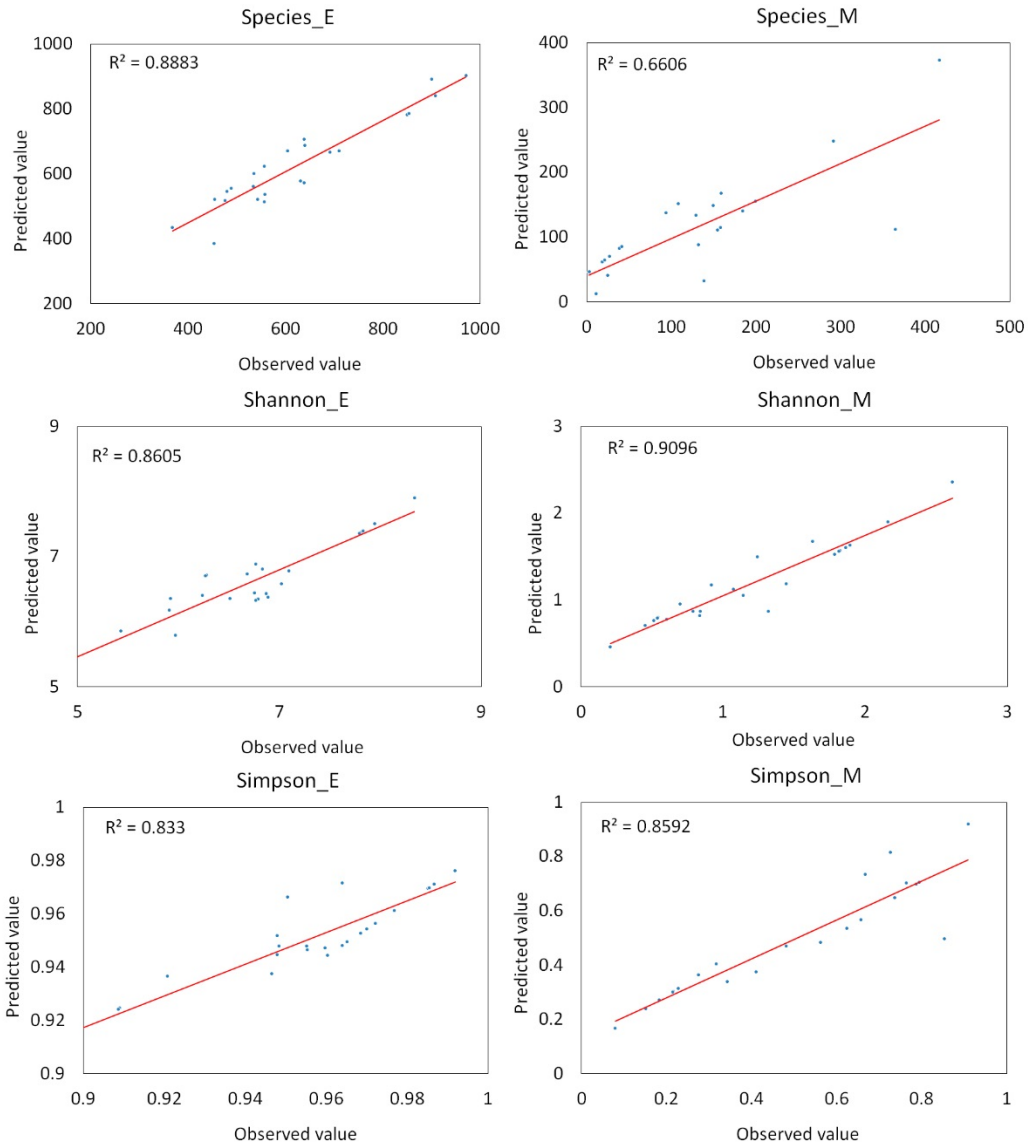
361

362 **Fig. 4.** Comparison of the three ecological index values derived from eDNA
 363 metabarcoding and morphology identification data.

364

365 3.2. Predictive performances and sensitivity analysis of SVM models

366 After optimizing the model parameters ($c = 10000$, $\varepsilon = 0.2$, and $\gamma = 0.025$) according
 367 to the methodology presented in Subsection 2.4, the nonlinear regression analysis
 368 results obtained by the SVM models for the three indices (Species_E, Shannon_E,
 369 Simpson_E) derived from eDNA metabarcoding data and the three indices (Species_M,
 370 Shannon_M, Simpson_M) derived from morphological identification data are
 371 presented in Fig. 5. The results indicated that, with the exception of Species_M (squared
 372 correlation coefficient $R^2 = 0.66$), the SVM models achieved good prediction
 373 performance, with R^2 values that were all greater than 0.80.



374

375 **Fig. 5.** Nonlinear regression fitting plots of the support vector machine (SVM) models
 376 for the measured values and predicted values of the three ecological indices.

377

378 The minimum values of MAPE for all samples (MAPE_ALL) and the minimum
 379 values of MAPE for the test samples (MAPE_TEST) obtained by 8-fold cross-
 380 validation indicated the accuracy of different models (Table 3). The results indicated
 381 that the MAPE_ALL values of the three most accurate SVM models obtained from
 382 eDNA metabarcoding data were in the order of Species_E > Shannon_E > Simpson_E,
 383 and the MAPE_ALL values of the three most accurate SVM models obtained from

384 morphology identification data exhibited an equivalent pattern. Nevertheless, the SVM
 385 models constructed from the eDNA metabarcoding data had MAPE values that were
 386 much smaller than those of the models constructed from the morphological
 387 identification data whether based on MAPE_ALL or MAPE_TEST values. This
 388 indicated that the models constructed from eDNA metabarcoding data were more
 389 accurate than those constructed from the morphological identification data.

390

391 **Table 3**

392 Results of model selection using 8-fold cross-validation for each ecological index given
 393 in terms of the minimum values of MAPE for all samples (MAPE_ALL), and the
 394 minimum values of MAPE for the test samples (MAPE_TEST).

Ecological index	MAPE_ALL	MAPE_TEST
Index derived from eDNA metabarcoding data		
Species_E	9.06	6.72
Shannon_E	5.14	4.14
Simpson_E	1.33	0.75
Index derived from morphology identification data		
Species_M	183.96	49.57
Shannon_M	25.61	15.50
Simpson_M	25.37	20.00

395

396 The sensitivity of each ecological index to multiple stressors were varying (Table 4).
 397 For Species_E, the largest value of Δ MAPE = 1.12 was obtained for SS, indicating that
 398 the Species_E prediction was most sensitive to this variable. For Shannon_E, the largest
 399 value of Δ MAPE = 0.47 was obtained for SS, indicating that the Shannon_E prediction
 400 was most sensitive to this variable. For Simpson_E, the largest value of Δ MAPE = 0.05
 401 was obtained for DO, indicating that the Simpson_E prediction was most sensitive to

402 this variable. Likewise, we can determine that the Species_M prediction was most
 403 sensitive to DO ($\Delta\text{MAPE} = 21.79$), the Shannon_M prediction was most sensitive to
 404 VP ($\Delta\text{MAPE} = 2.17$), and the Simpson_M prediction was most sensitive to VP
 405 ($\Delta\text{MAPE} = 2.13$). We also note from Table 4 that the magnitudes of the ΔMAPE values
 406 for the ecological indices obtained from DNA metabarcoding data are much smaller
 407 than those obtained from morphological identification data.

408

409 **Table 4**

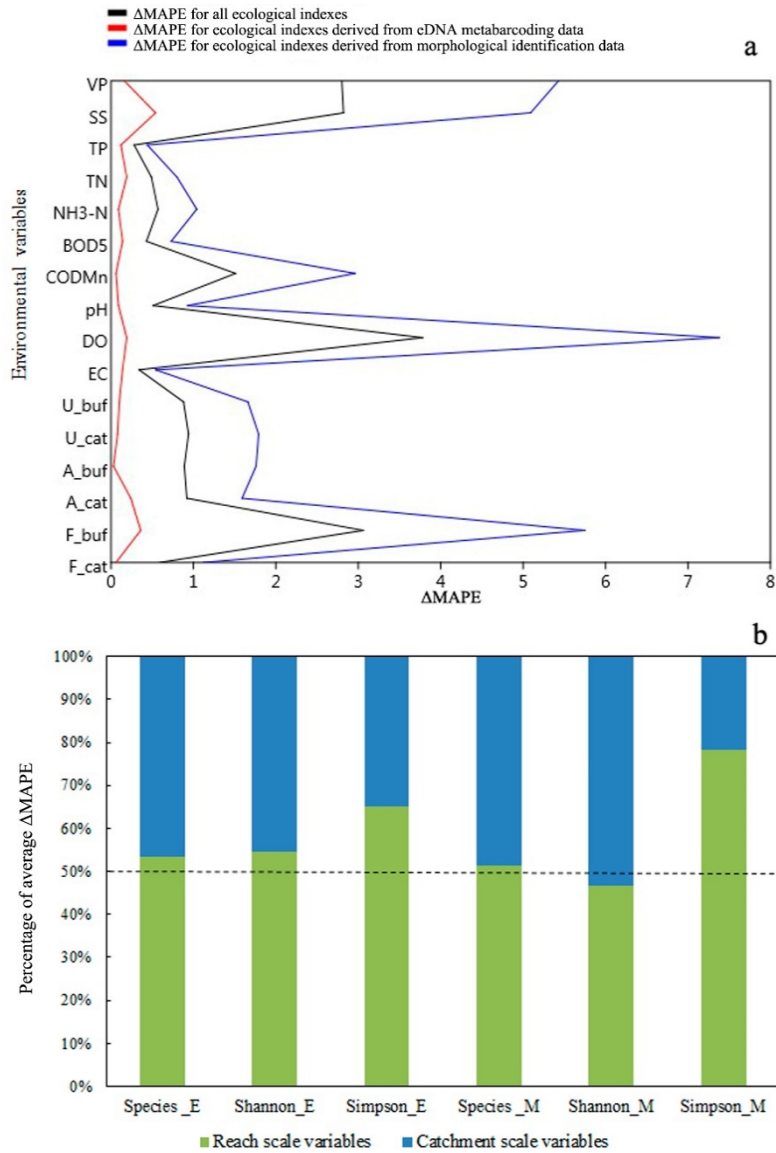
410 Results of sensitivity analysis based on the change in MAPE values (ΔMAPE) for all
 411 samples with respect to the individual environmental variables.

Environmental variables	Species	Shannon_	Simpson_	Species	Shannon_	Simpson_
	_E	E	E	_M	M	M
ΔMAPE						
Catchment-scale variables						
F_cat	0.13	0.04	0	3.19	0.16	0.02
F_buf	0.62	0.44	0.03	15.47	1.59	0.18
A_cat	0.62	0.09	0	3.69	0.78	0.31
A_buf	0	0.07	0.01	4.67	0.55	0.07
U_cat	0.1	0.11	0.04	4.87	0.07	0.42
U_buf	0.29	0.01	0	4.2	0.62	0.16
Reach-scale variables						
EC	0.36	0.02	0.03	1.34	0.15	0.14
DO	0.16	0.35	0.05	21.79	0.06	0.29
pH	0.15	0.08	0.03	1.84	0.68	0.28
COD _{Mn}	0.14	0.04	0	8.27	0.13	0.47
BOD ₅	0.24	0.16	0.02	0.68	0.11	1.39
NH ₃ -N	0.22	0.02	0.03	2.01	0.32	0.8
TN	0.34	0.19	0.04	0.63	1.12	0.64

TP	0.28	0.07	0.01	0.8	0.05	0.47
SS	1.12	0.47	0.02	14.22	0.72	0.34
VP	0.35	0.12	0.02	11.99	2.17	2.13

412

413 The variations in the Δ MAPE values for the ecological indices obtained from DNA
414 metabarcoding and morphological identification data are more clearly shown in Fig.
415 6A. We note that, among all six ecological indices, DO, SS, and VP are the three
416 environmental variables in the reach scale that most greatly affect the index value
417 predictions. These are followed by F_buf, the variable in the catchment scale. A
418 comparison of the average Δ MAPE values obtained for the environmental variables
419 shown in Fig. 6B indicate that, with the exception of Shannon_M, the environmental
420 variables at the reach scale have a greater impact on the ecological indices than those
421 at the catchment scale.



422

423 **Fig. 6.** (a) Δ MAPE values for each environmental variable in the sensitivity analysis

424 and (b) a comparison of sensitivities between catchment and reach scale environmental

425 variables.

426

427 4. Discussion

428 4.1. SVM model development and validation

429 The SVM models increase our understanding of the non-linear relationships between

430 ecological status and multiple stressors on the one hand and the sensitivity of the

431 ecological status to each stressor on the other. More importantly, the MAPE and high

432 R^2 values obtained by the SVM models demonstrate quantitatively that eDNA
433 metabarcoding data provide modeling results that were more indicative of
434 environmental degradation compared with morphological identification data. However,
435 we must note that OTUs contained more taxa information than species, which may
436 increase the uncertainty of the model comparison. However, the greater the number of
437 OTUs does not necessarily mean the better model performance, because a larger data
438 may also bring noise for modeling (Lu et al., 2018). In many biodiversity surveys and
439 assessments, the concept of OTUs diversity has been roughly equated with the concept
440 of species diversity (Caron and Hu, 2019), because OTUs use 3% sequence difference
441 to distinguish species, which is an accepted standard in molecular biology techniques
442 (Schloss and Handelsman, 2005). Previous study also showed that eDNA
443 metabarcoding and morphological macroinvertebrate metrics are positively correlated
444 and indicate the same key gradients in stream condition (Emilsson et al., 2017).

445 Furthermore, this kind of uncertainty can be reduced by using some ecological
446 indices (e.g. the Simpson and Shannon-Weiner indices), which represent the relative
447 diversity of taxa. These indices have all been normalized before modeling, and the
448 results showed that the normalized values of these ecological indices are relatively
449 consistent in most sampling sites (Fig. 4). Therefore, the uncertainty of the model due
450 to different classification levels can be reduced. In addition, our results were obtained
451 with a relatively small training dataset, and increasing the number of samples or
452 applying a larger sampling area can lead to the process of refining our predictive models.
453 This is supported by a previous study, which has shown that the accuracy and stability
454 of predictions increased exponentially with increasing sample size regardless of the
455 type of ML algorithm adopted (Cui and Gong, 2018).

456

457 *4.2. Ecological response derived from eDNA metabarcoding and morphological*
458 *identification data to multiple stressors*

459 Although the ecological indices obtained from morphological identification data
460 exhibited good response relationships with multi-scale stressors, the models
461 constructed from eDNA metabarcoding data provided better accuracy, as shown in
462 Table 3. This is because the effective eDNA sequencing information includes a large
463 number of intact and fragmentary organisms, and even includes the DNA information
464 of many historically existing organisms. This is supported by a previous study, which
465 found that the DNA information of some species may exist in water for up to one month
466 after the removal of DNA release sources (Li et al., 2018b). In addition, it has been
467 shown that eDNA metabarcoding data provide more integral information regarding
468 biology, including the taxa and even the potential bioindicators of pollution, for
469 example, the OTUs that dominate eDNA datasets in high mercury concentration do not
470 need to be assigned taxonomically, which are typically overlooked in morphological
471 identification (Frontalini et al., 2018). In conclusion, the biodiversity information
472 contained in eDNA data is massive, and the large volume of data available may alleviate
473 model prediction uncertainties caused by sample size limitations to some extent.

474 It is worth noting that eDNA metabarcoding data are not able to provide some
475 information available from morphological identification data. For example, eDNA
476 metabarcoding data provides no information regarding the morphological deformations
477 of target organisms, which are often found in highly polluted environments, and are
478 commonly used as evidence for heavy metal pollution (Yanko et al., 1998). Therefore,
479 eDNA metabarcoding data cannot replace morphological analysis when studying the
480 response of a particular species, but methods to detect change population of one or
481 multiple organisms to environmental stressors by eDNA metabarcoding are developing,

482 such as screening for functional genes, which may enable the eDNA metabarcoding to
483 assess toxicological information (Zhang et al., 2019). This will widen the application
484 of eDNA metabarcoding in environmental sciences.

485

486 *4.3. Sensitivity differences with respect to catchment and reach scale stressors*

487 The sensitivity analysis results indicated that DO, SS, VP, and F_buf have the greatest
488 impact on the model predictions of diversity indices, and that environmental variables
489 at the reach scale are more influential than that at the catchment scale, as shown in Table
490 4 and Fig. 6. This greater sensitivity of ecological status to reach-scale stressors can be
491 explained by noting that disturbances in land use at the catchment scale affect the
492 aquatic ecological status by generating non-point source pollutants, such as fertilizers,
493 pesticides, and sewage irrigation, that enter water bodies, resulting in increased
494 nutrition, bacteria, toxicity, and harmful substances, which means that the changes at
495 the reach scale affect the ecological status of rivers directly (Meador and Goldstein,
496 2003; Piggott et al., 2012).

497 The DO is directly decreased under these degrading conditions (Mineau et al., 2015)
498 Moreover, DO has been shown to be a key variable impacting the status of many aquatic
499 species because it can affect the tolerance limit of organisms (Marshall and Elliott,
500 1998). In addition, sites with the highest DO level have also been shown to have the
501 highest aquatic species diversity (Wilhm and McClintock, 1978). A previous study has
502 also demonstrated that SS is critical to phytoplankton communities because
503 phytoplankton growth requires photosynthesis, and light intensity in the photic zone
504 has a significant negative correlation with SS (Van Duin et al., 2001). Finally, we note
505 that urban and industrial land use in the urban section of the study area increased
506 significantly since the work of (Fan et al., 2015), and this can be expected to have

507 released toxic chemicals from industrial pollution, such as VP, into water bodies. In this
508 regard, the photosynthetic activity parameters of algae have been shown to have a
509 negative dose-response relationship to phenol toxicity (Kottuparambil et al., 2014).
510 Therefore, VP represents another critical environmental variable impacting the status
511 of many aquatic species.

512

513 **5. Conclusion**

514 The present study compared the ability of eDNA metabarcoding data and
515 morphological identification data to reflect the nonlinear impact of multiple
516 environmental stressors on aquatic ecosystems by employing both sets of data in SVM
517 models corresponding to three ecological indices (i.e. observed species, Shannon
518 Wiener index, and Simpson index). Analysis of the environmental variables at the
519 catchment and reach scales of the study area indicated that most of the variables
520 exceeded their natural thresholds at some of the sampling sites, and became a complex
521 of simultaneously interacting stressors affecting the ecological status of the river. The
522 SVM models constructed from eDNA metabarcoding data (MAPE = 3.87) provided
523 more accurate predictions than the SVM models constructed from morphological
524 identification data (MAPE = 28.36), revealing that the eDNA metabarcoding data better
525 reflected ecological conditions. As such, the present work helps to explore the potential
526 applications of eDNA technology in the monitoring and management of aquatic
527 ecosystems. In addition, the sensitivity of SVM model predictions of aquatic ecosystem
528 diversity to catchment-scale and reach-scale stressors was evaluated, and the stressors
529 having the greatest impact on the ecological status of rivers were identified. These
530 results indicated that the model predictions were more sensitive to the environmental
531 variables at the reach scale than those at the catchment scale. In addition, DO, SS, VP,

532 and F_buf were found to be the most influential variables impacting the ecological
533 status of the river.

534

535 **Acknowledgments**

536 The authors thank Dr. Xuwang Yin and Dr. Jianing Lin for their taxonomic experts
537 consultation on morphological identification. The authors also thank the anonymous
538 referees for their valuable comments regarding the manuscript.

539

540 **Funding**

541 This work was financially supported by the Fundamental Research Funds for Central
542 Public Welfare Scientific Research Institutes of China (Grant No. 2019YSKY-021), and
543 the Major Science and Technology Program for Water Pollution Control and Treatment
544 (Grant No. 2017ZX07301002-01).

545

546 **References**

547 Al-Mukhtar, M., 2019. Random forest, support vector machine, and neural networks to
548 modelling suspended sediment in Tigris River-Baghdad. *Environmental Monitoring
549 and Assessment* 191 (11), 673. <https://doi.org/10.1007/s10661-019-7821-5>.

550 Amaral-Zettler, L.A., McCliment, E.A., Ducklow, H.W. and Huse, S.M., 2009. A
551 method for studying protistan diversity using massively parallel sequencing of V9
552 hypervariable regions of small-subunit ribosomal RNA genes. *PLoS One* 4 (7),
553 e6372. <https://doi.org/10.1371/journal.pone.0006372>.

554 Balfer, J. and Bajorath, J., 2015. Systematic artifacts in support vector regression-based
555 compound potency prediction revealed by statistical and activity landscape analysis.
556 *PLoS One* 10 (3), e0119301. <https://doi.org/10.1371/journal.pone.0119301>.

557 Bernhardt, E.S., Lutz, B.D., King, R.S., Fay, J.P., Carter, C.E., Helton, A.M., Campagna,
558 D. and Amos, J., 2012. How many mountains can we mine? Assessing the regional
559 degradation of central Appalachian rivers by surface coal mining. *Environmental*
560 *Science & Technology* 46 (15), 8115–8122. <https://doi.org/10.1021/es301144q>.

561 Bouboulis, P., Theodoridis, S., Mavroforakis, C. and Evaggelatos-Dalla, L., 2015.
562 Complex support vector machines for regression and quaternary classification. *IEEE*
563 *Transactions on Neural Networks and Learning Systems* 26 (6), 1260–1274.
564 <https://doi.org/10.1109/TNNLS.2014.2336679>.

565 Caporaso, J.G., Kuczynski, J., Stombaugh, J., Bittinger, K., Bushman, F.D., Costello,
566 E.K., Fierer, N., Pena, A.G., Goodrich, J.K., Gordon, J.I., Huttley, G.A., Kelley, S.T.,
567 Knights, D., Koenig, J.E., Ley, R.E., Lozupone, C.A., McDonald, D., Muegge, B.D.,
568 Pirrung, M., Reeder, J., Sevinsky, J.R., Turnbaugh, P.J., Walters, W.A., Widmann, J.,
569 Yatsunenko, T., Zaneveld, J. and Knight, R., 2010. QIIME allows analysis of high-
570 throughput community sequencing data. *Nature Methods* 7 (5), 335–336.
571 <https://doi.org/10.1038/nmeth.f.303>.

572 Caron, D.A. and Hu, S.K., 2019. Are we overestimating protistan diversity in nature?
573 *Trends in Microbiology* 27 (3), 197–205. <https://doi.org/10.1016/j.tim.2018.10.009>.

574 Cherkassky, V. and Ma, Y.Q., 2004. Practical selection of SVM parameters and noise
575 estimation for SVM regression. *Neural Networks* 17 (1), 113–126.
576 [https://doi.org/10.1016/S0893-6080\(03\)00169-2](https://doi.org/10.1016/S0893-6080(03)00169-2).

577 Choubin, B., Darabi, H., Rahmati, O., Sajedi-Hosseini, F. and Klove, B., 2018. River
578 suspended sediment modelling using the CART model: a comparative study of
579 machine learning techniques. *Science of the Total Environment* 615, 272–281.
580 <https://doi.org/10.1016/j.scitotenv.2017.09.293>.

581 Cordier, T., Esling, P., Lejzerowicz, F., Visco, J., Ouadahi, A., Martins, C., Cedhagen,

582 T. and Pawlowski, J., 2017. Predicting the ecological quality status of marine
583 environments from eDNA metabarcoding data using supervised machine learning.
584 *Environmental Science & Technology* 51 (16), 9118–9126.
585 <https://doi.org/10.1021/acs.est.7b01518>.

586 Cui, Z.X. and Gong, G.L., 2018. The effect of machine learning regression algorithms
587 and sample size on individualized behavioral prediction with functional connectivity
588 features. *Neuroimage* 178, 622–637.
589 <https://doi.org/10.1016/j.neuroimage.2018.06.001>.

590 De Vargas, C., Audic, S., Henry, N., Decelle, J., Mahé, F., Logares, R., Lara, E., Berney,
591 C., Le Bescot, N. and Probert, I., 2015. Eukaryotic plankton diversity in the sunlit
592 ocean. *Science* 348 (6237), 1261605. <https://doi.org/10.1126/science.1261605>.

593 Duong, T. T., Morin, S., Herlory, O., Feurtet-Mazel, A., Coste, M., 2008. Seasonal
594 effects of cadmium accumulation in periphytic diatom communities of freshwater
595 biofilms. *Aquatic Toxicology* 90, 19–28. [https://doi.org/](https://doi.org/10.1016/j.aquatox.2008.07.012)
596 [10.1016/j.aquatox.2008.07.012](https://doi.org/10.1016/j.aquatox.2008.07.012).

597 Edgar, R.C., 2013. UPARSE: highly accurate OTU sequences from microbial amplicon
598 reads. *Nature Methods* 10 (10), 996–998. <https://doi.org/10.1038/nmeth.2604>.

599 Emilson, C.E., Thompson, D.G., Venier, L.A., Porter, T.M., Swystun, T., Chartrand, D.,
600 Capell, S. and Hajibabaei, M., 2017. DNA metabarcoding and morphological
601 macroinvertebrate metrics reveal the same changes in boreal watersheds across an
602 environmental gradient. *Scientific Reports* 7, 1–11. [https://doi.org/10.1038/s41598-](https://doi.org/10.1038/s41598-017-13157-x)
603 [017-13157-x](https://doi.org/10.1038/s41598-017-13157-x).

604 Fan, J.T., Semenzin, E., Meng, W., Giubilato, E., Zhang, Y., Critto, A., Zabeo, A., Zhou,
605 Y., Ding, S. and Wan, J., 2015. Ecological status classification of the Taizi River
606 Basin, China: a comparison of integrated risk assessment approaches. *Environmental*

607 Science and Pollution Research 22 (19), 14738–14754.
608 <https://doi.org/10.1007/s11356-015-4629-x>.

609 Fernandez, S., Rodriguez, S., Martinez, J.L., Borrell, Y.J., Ardura, A. and Garcia-
610 Vazquez, E., 2018. Evaluating freshwater macroinvertebrates from eDNA
611 metabarcoding: a river Nalón case study. *PLoS One* 13 (8), e0201741.
612 <https://doi.org/10.1371/journal.pone.0201741>.

613 Franzo, A. and Del Negro, P., 2019. Functional diversity of free-living nematodes in
614 river lagoons: can biological traits analysis (BTA) integrate traditional taxonomic-
615 based approaches as a monitoring tool? *Marine Environmental Research* 145, 164–
616 176. <https://doi.org/10.1016/j.marenvres.2019.02.015>.

617 Frontalini, F., Greco, M., Di Bella, L., Lejzerowicz, F., Reo, E., Caruso, A., Cosentino,
618 C., Maccotta, A., Scopelliti, G. and Nardelli, M.P., 2018. Assessing the effect of
619 mercury pollution on cultured benthic foraminifera community using morphological
620 and eDNA metabarcoding approaches. *Marine Pollution Bulletin* 129 (2), 512–524.
621 <https://doi.org/10.1016/j.marpolbul.2017.10.022>.

622 He, X., Sutherland, T.F., Pawlowski, J. and Abbott, C.L., 2019. Responses of
623 foraminifera communities to aquaculture-derived organic enrichment as revealed by
624 environmental DNA metabarcoding. *Molecular Ecology* 28 (5), 1138–1153.
625 <https://doi.org/10.1111/mec.15007>.

626 Hering, D., Borja, A., Jones, J.I., Pont, D., Boets, P., Bouchez, A., Bruce, K., Drakare,
627 S., Hänfling, B. and Kahlert, M., 2018. Implementation options for DNA-based
628 identification into ecological status assessment under the European Water
629 Framework Directive. *Water Research* 138, 192–205.
630 <https://doi.org/10.1016/j.watres.2018.03.003>.

631 Hu, H.J. and Wei, Y.X. (2006) *The Freshwater Algae of China, Systematics, Taxonomy*

632 and Ecology, Science Press, Beijing.

633 Humbert, J.-F., Quiblier, C. and Gugger, M., 2010. Molecular approaches for
634 monitoring potentially toxic marine and freshwater phytoplankton species.
635 *Analytical and Bioanalytical Chemistry* 397 (5), 1723–1732.
636 <https://doi.org/10.1007/s00216-010-3642-7>.

637 Jarman, S.N., Berry, O. and Bunce, M., 2018. The value of environmental DNA
638 biobanking for long-term biomonitoring. *Nature Ecology & Evolution* 2 (8), 1192–
639 1193. <https://doi.org/10.1038/s41559-018-0614-3>.

640 Ji, Y.Q., Ashton, L., Pedley, S.M., Edwards, D.P., Tang, Y., Nakamura, A., Kitching, R.,
641 Dolman, P.M., Woodcock, P. and Edwards, F.A., 2013. Reliable, verifiable and
642 efficient monitoring of biodiversity via metabarcoding. *Ecology Letters* 16 (10),
643 1245–1257. <https://doi.org/10.1111/ele.12162>.

644 Jones, F.C., Plewes, R., Murison, L., MacDougall, M.J., Sinclair, S., Davies, C., Bailey,
645 J.L., Richardson, M. and Gunn, J., 2017. Random forests as cumulative effects
646 models: a case study of lakes and rivers in Muskoka, Canada. *Journal of*
647 *Environmental Management* 201, 407–424.
648 <https://doi.org/10.1016/j.jenvman.2017.06.011>.

649 Kefford, B.J., Marchant, R., Schäfer, R.B., Metzeling, L., Dunlop, J.E., Choy, S.C. and
650 Goonan, P., 2011. The definition of species richness used by species sensitivity
651 distributions approximates observed effects of salinity on stream macroinvertebrates.
652 *Environmental Pollution* 159 (1), 302–310.
653 <https://doi.org/10.1016/j.envpol.2010.08.025>.

654 Keylock, C.J., 2005. Simpson diversity and the Shannon–Wiener index as special cases
655 of a generalized entropy. *Oikos* 109 (1), 203–207. <https://doi.org/10.1111/j.0030-1299.2005.13735.x>.

656

657 Kottuparambil, S., Kim, Y.J., Choi, H., Kim, M.S., Park, A., Park, J., Shin, W. and Han,
658 T., 2014. A rapid phenol toxicity test based on photosynthesis and movement of the
659 freshwater flagellate, *Euglena agilis* Carter. *Aquatic Toxicology* 155, 9–14.
660 <https://doi.org/10.1016/j.aquatox.2014.05.014>.

661 Laroche, O., Wood, S.A., Tremblay, L.A., Ellis, J.I., Lejzerowicz, F., Pawlowski, J.,
662 Lear, G., Atalah, J. and Pochon, X., 2016. First evaluation of foraminiferal
663 metabarcoding for monitoring environmental impact from an offshore oil drilling
664 site. *Marine Environmental Research* 120, 225–235.
665 <https://doi.org/10.1016/j.marenvres.2016.08.009>.

666 Li, F., Peng, Y., Fang, W., Altermatt, F., Xie, Y., Yang, J. and Zhang, X., 2018a.
667 Application of environmental DNA metabarcoding for predicting anthropogenic
668 pollution in rivers. *Environmental Science & Technology* 52 (20), 11708–11719.
669 <https://doi.org/10.1021/acs.est.8b03869>.

670 Li, M., Shan, X.J., Wang, W.J., Dai, F.Q., Lu, D. and Wu, H.H., 2018b. Study on the
671 retention time of environmental DNA of *fenneropenaeus chinensis* in water. *Progress*
672 *in Fishery Sciences*, <https://doi.org/10.19663/j.issn2095-9869.20180906005>.

673 Lu, X.J., Ming, L., Liu, W.B. and Li, H.X., 2018. Probabilistic regularized extreme
674 learning machine for robust modeling of noise data. *IEEE Transactions on*
675 *Cybernetics* 48 (8), 2368–2377. <https://doi.org/10.1109/TCYB.2017.2738060>.

676 Marshall, S. and Elliott, M., 1998. Environmental influences on the fish assemblage of
677 the Humber estuary, UK. *Estuarine, Coastal and Shelf Science* 46 (2), 175–184.
678 <https://doi.org/10.1006/ecss.1997.0268>.

679 Marvuglia, A., Kanevski, M. and Benetto, E., 2015. Machine learning for toxicity
680 characterization of organic chemical emissions using USEtox database: learning the
681 structure of the input space. *Environment International* 83, 72–85.

682 <https://doi.org/10.1016/j.envint.2015.05.011>.

683 Meador, M.R. and Goldstein, R.M., 2003. Assessing water quality at large geographic
684 scales: relations among land use, water physicochemistry, riparian condition, and
685 fish community structure. *Environmental Management* 31 (4), 0504–0517.
686 <https://doi.org/10.1007/s00267-002-2805-5>.

687 Meissner, T., Sures, B. and Feld, C.K., 2019. Multiple stressors and the role of
688 hydrology on benthic invertebrates in mountainous streams. *Science of the Total
689 Environment* 663, 841–851. <https://doi.org/10.1016/j.scitotenv.2019.01.288>.

690 Mineau, M.M., Wollheim, W.M. and Stewart, R.J., 2015. An index to characterize the
691 spatial distribution of land use within watersheds and implications for river network
692 nutrient removal and export. *Geophysical Research Letters* 42 (16), 6688–6695.

693 Ministry of Water Resources, Quality Standards for Surface Water Resources.
694 http://www.mwr.gov.cn/zwgk/zfxxgkml/201301/t20130124_964289.html. (1994,
695 accessed 24 January 2013)

696 Mize, E.L., Erickson, R.A., Merkes, C.M., Berndt, N., Bockrath, K., Credico, J.,
697 Grueneis, N., Merry, J., Mosel, K. and Tuttle-Lau, M., 2019. Refinement of eDNA
698 as an early monitoring tool at the landscape-level: Study design considerations.
699 *Ecological Applications* 29 (6), e01951. <https://doi.org/10.1002/eap.1951>.

700 Mori, N., Debeljak, B., Skerjanec, M., Simcic, T., Kanduc, T. and Brancelj, A., 2019.
701 Modelling the effects of multiple stressors on respiration and microbial biomass in
702 the hyporheic zone using decision trees. *Water Research* 149, 9–20.
703 <https://doi.org/10.1016/j.watres.2018.10.093>.

704 Olson, J.R., 2018. Predicting combined effects of land use and climate change on river
705 and stream salinity. *Philosophical Transactions of the Royal Society B: Biological
706 Sciences* 374 (1764), 20180005. <https://doi.org/doi:10.1098/rstb.2018.0005>.

707 Park, Y., Cho, K.H., Park, J., Cha, S.M. and Kim, J.H., 2015. Development of early-
708 warning protocol for predicting chlorophyll-a concentration using machine learning
709 models in freshwater and estuarine reservoirs, Korea. *Science of the Total*
710 *Environment* 502, 31–41. <https://doi.org/10.1016/j.scitotenv.2014.09.005>.

711 Pawlowski, J., Kelly-Quinn, M., Altermatt, F., Apothéloz-Perret-Gentil, L., Beja, P.,
712 Boggero, A., Borja, A., Bouchez, A., Cordier, T. and Domaizon, I., 2018. The future
713 of biotic indices in the ecogenomic era: Integrating (e) DNA metabarcoding in
714 biological assessment of aquatic ecosystems. *Science of the Total Environment* 637,
715 1295–1310. <https://doi.org/10.1016/j.scitotenv.2018.05.002>.

716 Piette, E.R. and Moore, J.H., 2018. Improving machine learning reproducibility in
717 genetic association studies with proportional instance cross validation (PICV).
718 *BioData Mining* 11, 6. <https://doi.org/10.1186/s13040-018-0167-7>.

719 Piggott, J.J., Lange, K., Townsend, C.R. and Matthaei, C.D., 2012. Multiple stressors
720 in agricultural streams: a mesocosm study of interactions among raised water
721 temperature, sediment addition and nutrient enrichment. *PLoS One* 7 (11), e49873.
722 <https://doi.org/10.1371/journal.pone.0049873>.

723 Piggott, J.J., Townsend, C.R. and Matthaei, C.D., 2015. Reconceptualizing synergism
724 and antagonism among multiple stressors. *Ecology and Evolution* 5 (7), 1538–1547.
725 <https://doi.org/10.1002/ece3.1465>.

726 Romero, F., Sabater, S., Timoner, X. and Acuña, V., 2018. Multistressor effects on river
727 biofilms under global change conditions. *Science of the Total Environment* 627, 1–
728 10. <https://doi.org/10.1016/j.scitotenv.2018.01.161>.

729 Rossel, R.A.V. and Behrens, T., 2010. Using data mining to model and interpret soil
730 diffuse reflectance spectra. *Geoderma* 158 (1–2), 46–54.
731 <https://doi.org/10.1016/j.geoderma.2009.12.025>.

732 Schloss, P.D. and Handelsman, J., 2005. Introducing DOTUR, a computer program for
733 defining operational taxonomic units and estimating species richness. *Applied and*
734 *Environmental Microbiology* 71 (3), 1501–1506.
735 <https://doi.org/10.1128/AEM.71.3.1501-1506.2005>.

736 Strong, W.L., 2016. Biased richness and evenness relationships within Shannon–
737 Wiener index values. *Ecological Indicators* 67, 703–713.
738 <https://doi.org/10.1016/j.ecolind.2016.03.043>.

739 Torija, A.J. and Ruiz, D.P., 2015. A general procedure to generate models for urban
740 environmental-noise pollution using feature selection and machine learning methods.
741 *Science of the Total Environment* 505, 680–693.

742 Treusch, A. H., Demirhilton, E., Vergin, K. L., Worden, A. Z., Carlson, C. A., Donatz,
743 M. G., ... & Giovannoni, S. J., 2012. Phytoplankton distribution patterns in the
744 northwestern Sargasso Sea revealed by small subunit rRNA genes from plastids. *The*
745 *ISME Journal*, 6(3), 481-492. <https://doi.org/10.1038/ismej.2011.117>

746 Van Duin, E.H.S., Blom, G., Los, F.J., Maffione, R., Zimmerman, R., Cerco, C.F.,
747 Dortch, M. and Best, E.P.H., 2001. Modeling underwater light climate in relation to
748 sedimentation, resuspension, water quality and autotrophic growth. *Hydrobiologia*
749 444 (1–3), 25–42. <https://doi.org/10.1023/A:1017512614680>.

750 Vapnik, V.N., 1999. An overview of statistical learning theory. *IEEE Transactions on*
751 *Neural Networks* 10 (5), 988–999. <https://doi.org/10.1109/72.788640>.

752 Varoquaux, G., 2018. Cross-validation failure: small sample sizes lead to large error
753 bars. *Neuroimage* 180 (Part A), 68–77.
754 <https://doi.org/10.1016/j.neuroimage.2017.06.061>.

755 Visco, J.A., Apotheloz-Perret-Gentil, L., Cordonier, A., Esling, P., Pillet, L. and
756 Pawlowski, J., 2015. Environmental monitoring: inferring the diatom index from

757 next-generation sequencing data. *Environmental Science & Technology* 49 (13),
758 7597–7605. <https://doi.org/10.1021/es506158m>.

759 Von Schiller, D., Acuna, V., Aristi, I., Arroita, M., Basaguren, A., Bellin, A., Boyero, L.,
760 Butturini, A., Ginebreda, A. and Kalogianni, E., 2017. River ecosystem processes: a
761 synthesis of approaches, criteria of use and sensitivity to environmental stressors.
762 *Science of the Total Environment* 596, 465–480.
763 <https://doi.org/10.1016/j.scitotenv.2017.04.081>.

764 Were, K., Bui, D.T., Dick, O.B. and Singh, B.R., 2015. A comparative assessment of
765 support vector regression, artificial neural networks, and random forests for
766 predicting and mapping soil organic carbon stocks across an Afrotropical landscape.
767 *Ecological Indicators* 52, 394–403. <https://doi.org/10.1016/j.ecolind.2014.12.028>.

768 Wilhm, J. and McClintock, N., 1978. Dissolved oxygen concentration and diversity of
769 benthic macroinvertebrates in an artificially destratified lake. *Hydrobiologia* 57 (2),
770 163–166. <https://doi.org/10.1007/BF00016460>.

771 Yanko, V., Ahmad, M. and Kaminski, M., 1998. Morphological deformities of benthic
772 foraminiferal tests in response to pollution by heavy metals: implications for
773 pollution monitoring. *The Journal of Foraminiferal Research* 28 (3), 177–200.

774 Yuan, J., Li, M. and Lin, S., 2015. An improved DNA extraction method for efficient
775 and quantitative recovery of phytoplankton diversity in natural assemblages. *PLoS*
776 *One* 10 (7), e0133060. <https://doi.org/10.1371/journal.pone.0133060>.

777 Zhang, L., Calvo-Bado, L., Murray, A.K., Amos, G.C.A., Hawkey, P.M., Wellington,
778 E.M. and Gaze, W.H., 2019. Novel clinically relevant antibiotic resistance genes
779 associated with sewage sludge and industrial waste streams revealed by functional
780 metagenomic screening. *Environment International* 132, 105120.
781 <https://doi.org/10.1016/j.envint.2019.105120>.

782 Zhang, X., 2019. Environmental DNA shaping a new era of ecotoxicological research.
783 Environmental Science & Technology 53 (10), 5605–5612.
784 <https://doi.org/10.1021/acs.est.8b06631>.

785

786

787